

HILDCAA* events between 1998 and 2007, and their related interplanetary magnetic field and plasma values

Alan Prestes

Vale do Paraiba University - UNIVAP 12244-000 São José dos Campos, SP, Brazil

Virginia Klausner*

Vale do Paraiba University - UNIVAP 12244-000 São José dos Campos, SP, Brazil

Arian Ojeda Gonzalez

Vale do Paraiba University - UNIVAP 12244-000 São José dos Campos, SP, Brazil

Silvio Leite Serra

Vale do Paraiba University - UNIVAP 12244-000 São José dos Campos, SP, Brazil

Abstract

We investigate the interplanetary conditions during 135 less strict high-intensity, long-duration, continuous AE activity (HILDCAA*) events between the years 1998–2007. The HILDCAA* events were chosen by following the three “traditional” criteria which describe the high-intensity, long-duration, continuous AE activity (HILDCAA). However, we include a small modification in the criteria that considers: “the AE values do not drop below 200 nT for more than 2 h at a time”. This criteria is modified by changing 2 to 4 hours period in which the AE values should not drop below 200 nT. Once the events are selected, we perform a statistical analysis of the interplanetary parameters during their occurrences. The distribution of HILDCAA* events along the solar cycle shows a pattern of double peak, with a peak around the maximum of the sunspot cycle, and an other in the descending phase. This kind of distribution is similar to the distribution of low-latitude coronal holes. For each of the HILDCAA* events, we have found its related Interplanetary Magnetic Field (IMF) and plasma parameter signatures. The average values of AE, AU, AL, and Dst indices, the density and temperature of the solar wind protons, the solar wind speed, the Bz component of the IMF, the IMF intensity, dynamic pressure, and plasma beta, among all the 135 HILDCAA* events, found here are: AE (348.1 ± 67.1 nT), AU (123.9 ± 34.2 nT), AL (-224.2 ± 47.3 nT), Dst (-22.1 ± 9.1 nT), Density (4.3 ± 1.3 cm⁻³), Temperature (170976.3 ± 58049.9 K), Flow speed (547.1 ± 83.9 km/s), Bz (-0.70 ± 0.88 nT), IMF magnitude average ($6.6 \pm$

*Corresponding author

Email addresses: prestes@univap.br (Alan Prestes), virginia@univap.br (Virginia Klausner), arian@univap.br (Arian Ojeda Gonzalez), silvio-serra@bol.com.br (Silvio Leite Serra)

1.2 nT), pressure (2.4 ± 0.6 nPa), and plasma Beta (0.66 ± 0.27).

Keywords: HILDCAAs*; Solar cycle; Interplanetary parameters; Table of events

1. Introduction

Different solar wind sources cause variations in the interplanetary medium, such as variations in density, speed, temperature, and interplanetary magnetic field (IMF). Upon reaching Earth magnetosphere, these variations generate disturbances in the magnetospheric and ionospheric current systems changing the geomagnetic field values measured on ground. Solar activity is responsible for many disturbances in the geomagnetic field that can be recurrent or transient. In general, there are basically 2 solar sources responsible for geomagnetic variation over a solar cycle. First: Interplanetary Coronal Mass Ejection (ICME) related magnetic storms near solar maximum, and second: Corotating Interaction Regions (CIR) storms during the solar minimum and its declining phase (Tsurutani and Gonzalez, 1987, 1997; Tsurutani et al., 1988, 1995; Gosling, 1993; Gonzalez et al., 1994; Suess and Tsurutani, 1998; Richardson et al., 2000; Echer et al., 2008). The solar activity varies over an 11-year period, therefore, the interplanetary medium structures and the interplanetary magnetic field also vary systematically according to the solar activity (Parks, 1991; Kivelson and Russell, 1995).

During minimum and descending solar activity, the possibility for geomagnetic disturbance is mainly due to the recurrent of coronal holes HSS (High Speed Stream). It is common that the coronal holes persist for more than one solar rotation (Sheeley et al., 1976, 1977; Tsurutani et al., 1995). Therefore, their recurring effects can be seen on Earth for several days or weeks, lasting up to an entire solar rotation about ~ 27 days (Tsurutani et al., 1995). High Speed Streams (HSSs) (Smith and Wolfe, 1976) are characterized by the presence of Alfvén waves propagating from the Sun (Belcher and Leverett, 1971; Shugai et al., 2009). Due to their fast velocity, the HSSs flow more radially from the Sun than the slow solar wind from other regions (Guarnieri et al., 2006).

Alfvén waves are often detected a few days after the CIRs, and they can last (but not always) for several days. The magnetic reconnection between the component in the southern direction of the magnetic field of Alfvén waves and the magnetospheric field is the mechanism to energy transfer between the solar wind and the Earth’s magnetosphere. Sometimes, High-Intensity Long-Duration Continuous AE Activity (HILDCAA) can occur (Tsurutani et al., 1995, 2004).

Tsurutani and Gonzalez (1987) defined HILDCAA events as intervals of: (1) High-Intensity - AE peak values exceed 1000 nT; (2) Long-Duration - the durations were greater than 2 days; (3) Continuous AE Activity - the AE values never dropped below 200 nT for more than 2 h at a time; and (4) HILDCAAs must occur outside of the main phase of magnetic storms. These criteria were imposed to illustrate the physical process related to the aforementioned solar energy transfer into the magnetosphere. However, the same physical process may occur even one or more of the four criteria are not strictly followed (Tsurutani et al., 2004).

Here, we are interested in analyzing the solar wind speed, density, intensity and orientation of the interplanetary magnetic field, and temperature during HILDCAA* events. During geomagnetically quiet periods, the solar wind flows at Earth’s orbit with speed of about 400 km/s and density of approximately 5 cm^{-3} , and it carries a magnetic field of about 5 nT. The solar wind controls the size of the magnetic cavity, through its dynamic pressure, and the energy flow into the magnetosphere by the magnetic reconnection of the interplanetary field with the terrestrial field (Dungey, 1961). The bow shock heats and compresses the magnetospheric plasma. It also compresses the magnetic field, so Alfvén waves in the HSS are amplified as they pass through the bow shock. Moreover, the southward component direction of the interplanetary magnetic field is amplified as well. If there are strong southward components within the CIR, a magnetic storm will happen (Dungey, 1961).

Moreover, we verify the effects of the interactions between the solar wind and the magnetosphere using the geomagnetic indices, AE and Dst, which are designed to represent the disturbance level of the Earth’s magnetosphere. Basically, the goal of any index is to provide information in a continuous manner about a more or less complex phenomena which varies with time. An index can be used for two purposes: to study the phenomenon itself, or as a reference to study an associated phenomenon (Mayaud, 1980). Here, we will use the AE and Dst indices to verify the associated interplanetary medium conditions.

2. Datasets and methodology

In this paper, we use the same methodology developed and evaluated by Prestes et al. (2016) to identify HILDCAAs* events. As discussed by Prestes et al. (2016), HILDCAA* events are defined by the following criteria: (1) AE peak values must exceed 1000 nT at least once during each event; (2) The event should last at least two days, (3) the AE values should never drop below 200 nT for periods longer than 4 hours at a time, and (4) HILDCAAs* must occur outside of the main phases of magnetic storms.

In order to determine the typical values of the solar wind parameters related to HILDCAA* events, we use ACE spacecraft data set with one-minute temporal resolution. The interplanetary solar wind data used here are: solar wind speed (V_{sw} in km/s), plasma density (N_{sw} in cm^{-3}), temperature (T_{sw} in K), flow pressure (P_{sw} in nPa), IMF magnitude (B_0 in nT), the B_x (nT), B_y (nT), B_z (nT) components in the GSM coordinate system, and plasma beta. We also use the AE, AU, and AL indices with one-minute temporal resolution, and the Dst index with one-hour resolution.

Figure 1 gives an example of “traditional” HILDCAA and HILDCAA* events. It is possible to notice that the HILDCAA event defined by Tsurutani and Gonzalez (1987) is entirely contained within a HILDCAA* event defined by Prestes et al. (2016) (event 10_1999). In this example, both events followed a geomagnetic storm. For this reason, the onset of HILDCAAs and/or HILDCAAs* is not taken until $Dst > -50$ nT, and consequently, these events occurred within the storm recovery phase. As discussed by Tsurutani and Gonzalez (1987), the recovery phase during this kind of events is much longer than usual and can last for more than a week as shown in Figure 1. In addition, it is possible to notice that the AE index shows intense and continuous activity.

Figure 2 shows all of the monthly HILDCAAs (top panel) and HILDCAAs* detected between 1998–2007. From this figure, it is seen an increase of the event numbers using the criteria defined by Prestes et al. (2016). On the top panel, there are only a few regions where there are many events. On the other hand, on the bottom panel this fact is not true, but the HILDCAA* events present the same variability of HILDCAA events according to the solar activity. There are a larger occurrence of HILDCAA and HILDCAA* during the declining phase (2003), a poor occurrence during the high solar activity (2001).

Following the criteria defined by Prestes et al. (2016), a total of 135 HILDCAA* events were found in the dataset from the years 1998 to 2007. The list of these events is presented in Table 1, which is arranged as follows: column 1 gives the studied events defined by numbers (from 1, 2, 3 and so forth...) and occurrence year; column 2 gives the starting date; column 3 gives the starting time in Universal Time (UT); column 4 gives the ending date; column 5 gives the ending time; and column 6 gives the preceding and/or associated interplanetary feature. In column 6, CIR stands for CIR magnetic storm preceding HILDCAA; CIR? stands for the possibility of CIR magnetic storm preceding HILDCAA; ICME stands for ICME magnetic storm preceding HILDCAA; ICME? stands for the possibility of ICME magnetic storm preceding HILDCAA; ICME+CIR stands for ICME and CIR magnetic storm preceding HILDCAA; ICME/CIR stands for ICME followed by CIR magnetic storm preceding HILDCAA; CIR/ICME stands for CIR followed by ICME magnetic storm preceding HILDCAA; CIR/ICME? stands for the possibility of CIR followed by ICME magnetic storm preceding HILDCAA; and ? indicates that any interplanetary feature was observed.

3. Results

Figure 3 shows the HILDCAA* events distribution, and the sunspot number variation over the years 1998–2007. Two peaks in the HILDCAA* distribution are observed in this figure. One: around the maximum of the sunspot cycle, and another: very intense in the descending phase of the cycle. The same kind of feature was observed by Hajra et al. (2013). From 135 HILDCAA* events occurring between 1998 and 2007, 47 ($\sim 35\%$) followed the storm main phase and occurred during the recovery phase. Figure 4 shows the number of HILDCAA* events which followed geomagnetic storms between the years of 1998 and 2007.

In addition, these 47 storm-associated HILDCAA events are highlighted in gray color in Table 1. The majority ($\sim 75\%$ – CIR (24 events), CIR? (4 events), ICME/CIR (3 events), CIR/ICME (3 events) and CIR+ICME (1 event)) of these storm-associated HILDCAA* events are associated with HSS. Approximately 10% of the cases (5 events) occurred after the passage of ICMEs. The remaining 15% could not be related to any interplanetary feature. Hajra et al. (2013) observed that 94% of storm-associated HILDCAA events were typically HSS-related, and consequently, associated with large interplanetary magnetic field (IMF) Bz variances. As discussed by Hajra et al. (2013), the small percentage of ICME-related HILDCAA events can be explained due to the small, steady southward Bz intervals or low-frequency fluctuations during the passage of these interplanetary features.

3.1. Statistical analysis

For each HILDCAA* event obtained for the period of 1998–2007, the following solar wind parameters are calculated using a statistical approach: proton density; proton temperature; solar wind speed and its components (V_x , V_y , V_z); magnetic field components (B_x , B_y , B_z); pressure and plasma beta; as well as the auroral geomagnetic indices: AE, AU, AL; and the low- to middle-latitude geomagnetic index: Dst. Histograms will be present next for all the aforementioned parameters calculated for ten consecutive years (1998–2007).

3.1.1. AE index

Figure 5 shows the distribution of AE index mean values for all 135 HILDCAAs* during 1998–2007. The average values for these events are above 213.75 nT for the whole period, and often they reach values above the double of the average value. The intensity range of the AE average is from a minimum of 224 nT to a maximum of 545 nT.

The majority of the AE average values occurs between 300–400 nT. In the year of 2003, there are 28 events, almost one every 10 days, and in this year, the AE index has an extremely high average of 328.26 nT, nearly 100 nT higher than the other years of the cycle 23, see Table 2. Coronal holes, as well HSSs and CIRs, are a possible source for explain this unusual average value.

3.1.2. AU/AL indices

Figure 6 shows the histograms of the average values of the AU and AL indices for 135 HILDCAA* events. For the AU index, we verify a minimum average of 51 nT and a maximum average of 214 nT.

In relation to the AL index during the HILDCAA* events, we verify a minimum average of -393 nT, and a maximum average of -146 nT. The largest number of events presents mean values of AL index between -250 to -150 nT.

3.1.3. Solar wind proton density

The average values of the solar wind proton density vary 1.9 cm^{-3} to 8.8 cm^{-3} , as noticed in Figure 7. Most of the events shows a density average lower than $6.1 \text{ particles per cm}^3$. This kind of results may be related to HSSs.

3.1.4. Solar wind proton temperature

The average values of the solar wind proton temperature presented a minimum of 48379 K and a maximum of 298180 K, see Figure 8. About 85% of the events has average values above 125000 K. Once more, this kind of results may be related to HSSs.

3.1.5. Solar wind speed

Among the 135 events, a minimum average value of the solar wind speed is 369 km/s and a maximum average is 715 km/s, as shown in Figure 9. The $\sim 85\%$ of the events has average values higher than whole period average which is $\approx 450 \text{ km/s}$. If we compare to the histogram of the solar wind speed derived from 18 months of ISSE-3 observations (see Russell, 2001, page 77, Figure 5) to the solar wind speed histogram in Figure 9, we verify

that the distribution of velocity during the occurrence of HILDCAA* events is shifted with respect to the most probable values, and they are above the level of 75% of the velocity quartiles.

3.1.6. Bz component of the interplanetary magnetic field

The Bz component of the interplanetary magnetic field shows mean values between -2.8 nT and 2.0 nT, see Figure 10. The distribution of Bz shows an almost a Gaussian distribution with a slight tendency to the left different from the distribution of Bz around zero observed by (Russell, 2001, page 82, Figure 23). However, when these values is compared to the Bz values during geomagnetic storms, we observe that the Bz during HILDCAAs* has smaller values than the average Bz values during storms, which is -3 nT for at least 1 hour (Gonzalez et al., 1994).

3.1.7. Magnitude of solar wind magnetic field

The distribution of average values for the interplanetary magnetic field magnitude B is shown in Figure 11. The occurrence interval of average is between 3.8 nT and 9.4 nT. However, the HILDCAA* events occur predominately in the range of 5 to 8 nT.

3.1.8. Solar wind dynamic pressure

In the years 1998–2007, during the occurrence of the HILDCAA* events, the dynamic pressure has values between 1.2 nPa and 4.5 nPa, as shown in the Figure 12. This histogram illustrates that the interval with the highest frequency of occurrences is between 1.5 to 3 nPa. The expected value of the solar wind dynamic pressure at Earth’s magnetosphere is about 2.6 nPa at any time of the solar cycle (Kivelson and Russell, 1995).

The dynamic pressure is similar to high-speed solar wind emerging from the coronal holes, and of low speed from streamer belt, which does not differ by more than 5%. Using only this kind of statistical solar wind dynamic pressure analysis, it is not possible to discern any stream structure. This means that both types of wind have the same dynamic pressure in any obstacle, for example, the planetary magnetospheres (Schwenn, 2006). Therefore, there are no significant differences in the distributions of the dynamic pressure during the occurrence of HILDCAA* events.

3.1.9. Solar wind plasma beta

The β parameter is the ratio of thermal pressure to magnetic pressure in the plasma. Fast streams have values closer to one, while other structures, such as magnetic clouds or CMEs, have the beta value much smaller than one. Plasma β values are between 0.15 and 2.08, see Figure 13. However, the β values are usually above 0.4 during the HILDCAA* events.

4. Summary and discussions

The distribution of HILDCAA* events throughout the solar cycle follows a distribution similar to that observed in the distribution of low-latitudes coronal holes during solar cycle 21, as found by (Gonzalez et al., 1996, see Figure 2.6). The existence of two peaks is also

observed here. One: less intense around the solar maximum, and another: more intense in the descending phase.

The time interval of the all analyzed HILDCAA* events varies approximately from 2 days to two weeks. During the descending phase of the solar cycle, there are an increase of HILDCAA* occurrences, and also, they persisted for longer time (see Table 1). The level of auroral activity, measured by the AE index, has a higher value during this phase, possibly due to the presence of long-term fast streams in the solar wind that originate from coronal holes. Peak values of AE index between 1000 and 2852 nT are found among all the 135 events, in the period from 1998 to 2007. The average values observed are between 224 and 545 nT.

Table 3 shows the mean values, with their corresponding standard deviations, for the AE, AU, AL, and Dst indices, density and temperature of the solar wind protons, solar wind speed, Bz component and intensity of the IMF, the dynamic pressure, and beta factor among all the 135 HILDCAA* events. Ahn and Moon (2003) analyzed the variations of the AU, AL, AE indices with an hourly time series from 1966 to 1987. They found average values for AU, AL, AE of 84.6 nT, -135.1 nT, and 213.7 nT (average for all period: both quiet and disturbed), respectively. For AL index, considering only disturbed period, $AL < -135$ nT, they found an average of -295.9 nT. The comparison between the values from Table 3 and values found by Ahn and Moon (2003) shows that AU during HILDCAA* events presents higher values, indicating that the eastward auroral electrojet, from which AU is derived, and it has higher disturbances during the occurrence of HILDCAA* events. The mean value of AL for HILDCAAs* is higher than during quiet periods, and lower than during perturbed periods.

Petrukovich and Rusanov (2005), who studied the dependence of the AL index in relation to various parameters of the solar wind and IMF, found that the variables with most influence are in order of importance: (1) electric field (VBs) and speed through viscous interaction; (2) By component, solar wind density (AL sensitive to low dynamic pressure), and intensity of IMF fluctuations. Here, both auroral electrojets, AU/AL, are disturbed during the occurrence of HILDCAA* events. This suggests that the two indices are modulated by the same mechanism, possibly by the electric field (Ahn et al., 2000; Ahn and Park, 2008).

The mean values of AE (348.1 nT), AU (123.9 nT), and AL (-224.2 nT) during HILDCAA* events reached relatively high levels if compared with a quiet period (with $AE \approx 50$ nT), and with their historical average values of 213.7 nT, 84.6 nT, and -135.1 nT, respectively (Ahn and Moon, 2003). The AU and AL indices have distributions similar to AE indicating that during HILDCAA* events both are energized. But it has been shown by Rostoker (1972); Baumjohann (1983); Kamide and Kokubun (1996) that the nature of eastward auroral electrojet (described by the AU) is quite different from the westward auroral electrojet (described by the AL). The AE index provides the sum of the maximum current density at two points that are also distant in local time. This sum has no physical meaning.

The parameters in the interplanetary medium during HILDCAA* events with highest average values are solar wind speed (547.1 km/s) and temperature (170976.3 K). Other parameters showed no significant changes, for example B (6.6 nT) and dynamic pressure (2.4

nPa). The B_z component has a negative average value (-0.70 nT). However, the expected value is zero. Therefore, the preferred direction for this component during HILDCAA* events is southward. Remembering that the magnetic reconnection occurs between the southward interplanetary magnetic field component and the geomagnetic field causing greater injection of energy into the magnetosphere (shown by [Guarnieri \(2005\)](#)).

The plasma beta is useful to identify solar wind structures such as magnetic clouds, shocks, and high-speed solar-wind streams, and it presents a relatively high average value of 0.66. Comparing this value to the values related to different structures in the interplanetary medium, the plasma beta is associated to high-speed solar-wind streams when its values are close to or larger than one. Other structures, such as magnetic clouds have a plasma beta values smaller than one. This analysis indicates that most events are associated to high-speed streams flowing from coronal holes. In many cases, these high speed streams are embedded into Alfvénic fluctuations covering a wide frequency bandwidth. The solar wind Alfvénicity has already been indicated by several authors as a possible cause of particle penetration, and particle precipitation ([Tsurutani and Gonzalez, 1987](#); [Tsurutani et al., 1995](#); [Tsurutani and Gonzalez, 1997](#); [Guarnieri, 2005](#)).

The distributions of the parameters related to the HILDCAA* events reveals that only 15 ($\sim 11\%$) of 135 events had average speeds higher than 650 km/s (see [Figure 9](#)). The histogram in [Figure 7](#) shows that 75% of events had an average density smaller than the average ($\approx 6.1 \text{ cm}^{-3}$) from 1998 to 2007. Therefore, a large compression from the solar wind to the magnetosphere is not observed for most of the events as seen by the low values of the dynamic pressure calculated for all events. However, it did not exceed 6 nPA, as shown in [Figure 12](#). For most HILDCAA* events, the average B_z component of the interplanetary magnetic field has mostly negative values (B_z is south) and a high average speed. Thus, the electric field E_y given by VBs has a component resulting in the dawn to dusk direction. This field configuration describes the energy transfer mechanism of the solar wind into the magnetosphere by magnetic reconnection, which is the most efficient mechanism to transfer energy ([Gonzalez et al., 1994](#)).

For a better understanding of results for the HILDCAA* events, we compare them to other periods in different conditions to have a reference between solar wind variations, and their seeding structures in the interplanetary medium.

As discussed by [Schwenn \(2006\)](#), there are two basic types of solar wind: slow wind and fast wind. These two kinds of solar wind differ markedly in their main properties, *i.e.*, in the location and the magnetic topology of their sources in the solar corona, and probably in the acceleration mechanism. Some characteristic values of the slow wind are: V_{sw} between 250–400 km/s, $N_{sw} \sim 10.7 \text{ cm}^{-3}$, $T_{sw} \sim 3.4 \times 10^4 K$, and their sources are found in the streamer belt in the solar corona. The characteristic values of the fast solar wind are: V_{sw} between 400–800 km/s, $N_{sw} \sim 3.0 \text{ cm}^{-3}$, $T_{sw} \sim 2.3 \times 10^5 K$, and their sources are in the coronal holes.

According to [Richardson et al. \(2000\)](#), the Earth passes about 10% of its time in solar wind structures related to CMEs at solar minimum phase, and 60% in solar wind structures related to corotating streams. At the solar maximum phase, the Earth passes about 30% of

its time in solar wind structures related to CMEs, and 30% in structures related to corotating streams. Thus, the Earth spends most of its time in solar wind structures related to fast streams.

Cane and Richardson (2003) studied 214 interplanetary coronal mass ejections (ICME), which occurred between 1996-2002, and they found average values of 454 ± 6 km/s for velocity and of 9.9 ± 0.3 nT for Bo. The mean speed of these events is less than the average of the HILDCAA* events. In addition, the average value of the interplanetary magnetic field is higher than the values related to HILDCAA* events. Thus, it can be inferred that HILDCAA* events are not associated with ICMEs.

Moreover, Gonzalez et al. (2011) found average values for Dst peak and some interplanetary parameters associated with superstorms. These values were Dst (-324.3 ± 67.3 nT), Vsw (799.1 ± 160.6 km/s), Bo (41.7 ± 10.8 nT), Bz (34.3 ± 13.5 nT), Ey (23.5 ± 11.6 mV/m), Nsw (24.7 ± 13.7 cm^{-3}), and Psw (25.7 ± 14.8 nPa). As can be seen, all parameters reached high values during superstorms.

The results presented and compared above elucidate that some parameters of magnetic field and of plasma of the interplanetary medium related to HILDCAA* events are intermediate values between periods of low geomagnetic activity (background values) and high geomagnetic activity values (storm values), as summarized in Table 4. Therefore with the parameters of plasma and IMF on hands, it is possible to determine which kind of geomagnetic event will occur.

5. acknowledgments

This research was supported by CNPq and FAPESP: A. Prestes FAPESP - (2009/02907-8) and CNPq (301441/2013-8). V. Klausner wishes to thank CNPq for the financial support for her postdoctoral research (grants 165873/2015-9). Furthermore, the authors would like to thank the WDC-Kyoto and OMNIWeb for the data sets used in this work. The AE and Dst indexes were obtained from the World Data Center for Geomagnetism - Kyoto (<http://wdc.kugi.kyoto-u.ac.jp/index.html>). The ACE parameters are available through the National Space Science Data Center (OMNIWeb):<http://omniweb.gsfc.nasa.gov/form/dx1.html>.

References

- Ahn, B.H.; Kroehl, H. W.; Kamide, Y.; Kihn, E. A. (2000), Seasonal and solar cycle variations of the auroral electrojet indices, *Journal of Atmospheric and Solar-Terrestrial Physics*, 62 (14), 1301–1310.
- Ahn, B.H.; Moon, G.H. (2003), Seasonal and Universal Time Variations of the AU, AL and Dst Indices, *Journal of the Korean Astronomical Society*, 36 (S1), S93–S99.
- Ahn, B.H.; Park, Y.K. (2008), Response of the Geomagnetic Activity Indices to the Solar Wind Parameters, *Journal Astron. Space Science*, 25 (2), 129–138.

- Baumjohann, W. (1983), Ionospheric and field-aligned current systems in the auroral zone, *Advances in Space Research.*, 2, 55–62.
- Belcher, J. W.; and D. Leverett (1971), Large-amplitude Alfvén waves in the interplanetary medium, 2, *Journal of Geophysical Research*, 76 (16), 3534–3563.
- Burlaga, L. F. (1988), Magnetic clouds and force-free fields with constant α , *Journal of Geophysical Research*, 93 (7), 7217–7224.
- Cane H. V.; Richardson I. G. (2003), Interplanetary coronal mass ejections in the near-Earth solar wind during 1996–2002, *Journal of Geophysical Research*, 108 (A4), 6.1–6.13.
- Dungey, J. W. (1961), Interplanetary Magnetic Field and the Auroral Zones, *Phys. Rev. Lett.* 6, 47.
- Echer, E.; Gonzalez, W. D.; Tsurutani, B. T.; and Gonzalez, A. L. C. (2008), Interplanetary conditions causing intense geomagnetic storms ($Dst \leq -100$ nT) during solar cycle 23 (1996–2006), *Journal of Geophysical Research: Space Physics*, 113 (A5), 2156–2202.
- Ergun, R. E., Andersson, L., Main, D., Su, Y.-J., Newman, D. L., Goldman, M. V., Carlson, C. W., Hull, A. J., McFadden, J. P., and Mozer, F. S. (2004), Auroral particle acceleration by strong double layers: The upward current region, *Journal of Geophysical Research: Space Physics*, 109 (A12), A12220.
- Gonzalez, W. D.; Clua de Gonzalez, A. L.; Tsurutani, B. T. (1992), Interplanetary magnetosphere coupling during intense geomagnetic storms at solar maximum, *Geofísica Internacional*, 31 (1), 11–18.
- Gonzalez, W. D., Joselyn, J. A., Kamide, Y., Kroehl, H. W., Rostoker, G., Tsurutani, B. T., Vasyliunas, V. M. (1994), What is a geomagnetic storm?, *Journal of Geophysical Research*, 99, 5771–5792.
- Gonzalez, W. D., Clua de Gonzalez, A. L., Sobral, J. H. A., Dal Lago, A., and Vieira, L. E. (1996), Solar and interplanetary causes of very intense geomagnetic storms, *J. Atm. Sol. Phys.*, 63, 403–412.
- Gonzalez, W. D., Echer, E., Tsurutani, B. T., Clua de Gonzalez, A. L., and Dal Lago, A. (2011), Interplanetary origin of intense, superintense and extreme geomagnetic storms, *Space Sci. Rev.*, 158, 69–89, doi:10.1007/s11214-010-9715-2.
- Gosling, J. T. (1993), Coronal mass ejections: The link between solar and geomagnetic activity, *Physics of Fluids B*, 5 (7), 2638–2645.
- Guarnieri, F. L. (2005), The Nature of Auroras During High-Intensity Long-Duration Continuous AE Activity (HILDCAA) Events: 1998 to 2001, *American Geophysical Union*, 235–243.

- Guarnieri, F. L., Tsurutani, B. T., Echer, E., Gonzalez, W. D. (2006), Geomagnetic Activity and Auroras Caused by High-Speed Streams: a Review, *Advances in Geosciences*, 8: Solar Terrestrial (ST) 8, 91–102.
- Hajra, R., Echer, E., Tsurutani, B. T., and Gonzalez, W. D. (2013), Solar cycle dependence of High-Intensity Long-Duration Continuous AE Activity (HILDCAA) events, relativistic electron predictors?, *Journal of Geophysical Research: Space Physics*, 118 (9), 5626–5638.
- Hsiao, G. C., E. P. Stephan, and W. L. Wendland (1991), On the Dirichlet problem in elasticity for a domain exterior to an arc, *J. Comput. Appl. Math.*, 34(1), 1–19.
- Kamide, Y.; Kokubun, S. (1996), Two component auroral electrojet: Importance for sub-storm studies, *Journal of Geophysical Research*, 101, 13027.
- Kivelson, M. G., and Russell, C. T. (1995), *Introduction to Space Physics*.
- Mayaud, P. N. (1980), *Derivation, Meaning, and Use of Geomagnetic Indices*, Washington DC, American Geophysical Union Geophysical Monograph Series 22, 607.
- Parks, G. K. (1991), *Physics of space plasmas - an introduction*.
- Petrukovich, A.A.; Rusanov, A.A. (2005), AL index dependence on the solar wind input revisited, *Advances in Space Research*, 36, 2440–2444.
- Prestes, A., V. Klausner, and A. O. Gonzalez (2016), Large number of HILDCAA* occurrences and an exceptionally high AE index average during 2003, Submitted to *Journal of Geophysical Research*, under revision 2016JA023406R (Editor - Michael Liemohn).
- Richardson, I. G., Cliver, E. W., and Cane, H. V. (2000), Sources of geomagnetic activity over the solar cycle: Relative importance of coronal mass ejections, high-speed streams, and slow solar wind, *Journal of Geophysical Research*, 105, 18203.
- Richardson, I. G., and Cane, H. V. (2012), Solar wind drivers of geomagnetic storms during more than four solar cycles, *J. Space Weather Space Clim.*, 2, A01.
- Rostoker, G. (1972), Geomagnetic indices, *Reviews of Geophysics and Space Physics*, 10 (4), 935–990.
- Russell, C. (2000), The solar wind interaction with the Earth’s magnetosphere: a tutorial.
- Russell, C. T. (2001), *Solar wind and interplanetary magnetic field: A tutorial*, Washington DC American Geophysical Union Geophysical Monograph Series 125, 73–89.
- Schwenn, R. (2006), Solar wind sources and their variations over the solar cycle, *Sp. Sc. Rev.*, 124, 51–76.
- Sheeley, N. R., Jr., J. W. Harvey, and W. C. Feldman (1976), Coronal holes, solar wind streams and recurrent geomagnetic disturbances: 1973-1976, *Sol. Phys.*, 49, 271.

- Sheeley, Jr., N.R., J.S. Asbridge, S.J. Bame, and J.W. Harvey (1977), A pictorial comparison of interplanetary magnetic field polarity, solar wind speed, and geomagnetic disturbance index during the sunspot cycle, *Solar Phys.*, 52, 485.
- Smith, E. J., and J. H. Wolfe (1976), Observations of interaction regions and corotating shocks between one and 5 AU-PIONEER-10 and PIONEER-11, *Geophys. Res. Lett.*, 3, 137–140, doi:10.1029/GL003i003p00137.
- Shugai, Y., Veselovsky, I., Trichtchenko, L. (2009), Studying correlations between the coronal hole area, solar wind velocity, and local magnetic indices in the Canadian region during the decline phase of cycle 23, *Geomagnetism and Aeronomy*, 49 (4), 415–424.
- Suess, S. T., and Tsurutani, B. T. (Eds.) (1998), *From the Sun, Auroras, Magnetic Storms, Solar Flares, Cosmic Rays*.
- Tsurutani, B. T., and Gonzalez, W. D. (1987), The cause of high-intensity long-duration continuous AE activity (HILDCAAS) - Interplanetary Alfvén wave trains, *Planetary and Space Science* 35, 405–412.
- Tsurutani, B. T., Smith, E. J., Gonzalez, W. D., Tang, F., and Akasofu, S. I. (1988), Origin of interplanetary southward magnetic fields responsible for major magnetic storms near solar maximum (1978-1979), *Journal of Geophysical Research*, 93, 8519–8531.
- Tsurutani, B. T., Gonzalez, W. D., Gonzalez, A. L. C., Tang, F., Arballo, J. K. and Okada, M. (1995), Interplanetary origin of geomagnetic activity in the declining phase of the solar cycle, *Journal of Geophysical Research: Space Physics*, 100 (A11), 2156–2202.
- Tsurutani, B. T. and Gonzalez, W. D. (1997), The Interplanetary Causes of Magnetic Storms: A Review, in *Magnetic Storms* (eds B. T. Tsurutani, W. D. Gonzalez, Y. Kamide and J. K. Arballo), American Geophysical Union, Washington, D. C.. doi: 10.1029/GM098p0077
- Tsurutani, B. T., Gonzalez, W. D., Guarnieri, F., Kamide, Y., Zhou, X., and Arballo, J. K. (2004), Are high-intensity long-duration continuous AE activity (HILDCAA) events substorm expansion events?, *Journal of Atmospheric and Solar-Terrestrial Physics* 66, 167–176.
- Tsurutani, B. T., Gonzalez, W. D., Gonzalez, A. L. C., Guarnieri, F. L., Gopalswamy, N., Grande, M., Kamide, Y., Kasahara, Y., Lu, G., Mann, I., McPherron, R., Soraas, F. and Vasyliunas, V. (2006), Corotating solar wind streams and recurrent geomagnetic activity: A review, *Journal of Geophysical Research: Space Physics*, 111 (A7), A07S01.
- Vennerstroem, S. (2001), Interplanetary sources of magnetic storms: A statistical study, *Journal of Geophysical Research* 106, 29175–29184.

Table 1: HILDCAA* events for the period between 1998-2007.

Event_Year	Start	UT	Stop	UT	Length (min)	Mechanism
01_1998	24 Apr	12:00	26 Apr	13:00	2940	CIR
02_1998	26 Apr	21:00	29 Apr	13:44	3884	?
03_1998	10 May	05:32	13 May	02:24	4132	?
04_1998	20 Jun	03:16	23 Jun	08:50	4654	CIR
05_1998	03 Jul	20:00	06 Jul	17:20	4160	CIR
06_1998	22 Jul	20:56	25 Jul	17:36	4120	CIR
07_1998	28 Aug	22:45	01 Sep	05:54	4749	ICME
08_1998	22 Sep	19:23	24 Sep	23:59	3156	ICME
09_1998	22 Oct	01:13	25 Oct	19:01	5388	ICME
01_1999	02 Mar	19:27	06 Mar	02:14	4727	CIR
02_1999	13 Mar	08:34	15 Mar	23:38	3785	?
03_1999	29 Mar	15:01	01 Apr	13:34	4233	CIR
04_1999	03 Apr	10:17	06 Apr	01:50	3813	?
05_1999	19 Apr	02:04	21 Apr	07:16	3192	?
06_1999	27 Apr	07:21	04 May	03:37	9856	CIR
07_1999	30 Jun	19:54	03 Jul	23:23	4529	ICME+CIR
08_1999	15 Aug	22:37	20 Aug	01:59	5962	CIR
09_1999	29 Aug	08:41	03 Sep	08:17	7176	?
10_1999	10 Oct	23:01	18 Oct	07:57	10615	CIR
11_1999	26 Oct	04:29	28 Oct	09:55	3206	CIR
12_1999	23 Nov	00:54	25 Nov	02:49	2995	CIR+ICME
13_1999	03 Dec	01:57	10 Dec	07:25	10408	CIR
01_2000	01 Jan	04:00	03 Jan	20:46	3886	CIR?
02_2000	04 Jan	05:46	07 Jan	21:18	5252	?
03_2000	27 Jan	18:06	31 Jan	23:01	6056	CIR
04_2000	05 Feb	15:53	08 Feb	22:16	4704	CIR
05_2000	24 Feb	02:42	27 Feb	21:37	5455	ICME/CIR
06_2000	06 Mar	05:07	09 Mar	01:03	4076	ICME/CIR
07_2000	30 Jul	11:11	02 Aug	12:42	4411	CIR
08_2000	04 Aug	00:16	07 Aug	13:24	5108	?
09_2000	30 Aug	20:39	01 Sep	22:59	3021	?
10_2000	06 Sep	15:02	09 Sep	00:18	3436	ICME
01_2001	06 Apr	06:37	11 Apr	12:30	7553	ICME
02_2001	10 May	11:00	14 May	08:47	5627	CIR
03_2001	09 Jun	04:00	11 Jun	05:49	2989	CIR
04_2001	15 Jul	06:19	18 Jul	08:57	4478	CIR

Continued on next page

Table 1 – continued from previous page

Event_Year	Start	UT	Stop	UT	Length (min)	Mechanism
05_2001	21 Jul	23:40	26 Jul	13:56	6617	CIR
06_2001	02 Sep	11:29	05 Sep	03:32	3843	CIR
07_2001	27 Sep	10:17	30 Sep	15:57	4660	?
08_2001	17 Nov	00:22	20 Nov	08:10	4788	?
01_2002	11 Jan	10:00	14 Jan	23:11	5111	CIR?
02_2002	06 Feb	11:00	09 Feb	13:09	4449	CIR
03_2002	05 Mar	00:41	07 Mar	01:05	2904	CIR/ICME
04_2002	14 May	13:00	17 May	00:01	3542	?
05_2002	08 Jun	12:06	12 Jun	05:25	5359	CIR
06_2002	22 Jul	01:35	24 Jul	11:58	3503	CIR+ICME
07_2002	24 Jul	18:49	28 Jul	06:12	5004	CIR+ICME
08_2002	13 Aug	07:00	16 Aug	17:19	4939	?
09_2002	09 Oct	01:01	13 Oct	13:08	6487	ICME/CIR
10_2002	25 Oct	21:00	29 Oct	15:33	3992	CIR
11_2002	29 Oct	20:30	01 Nov	01:48	3198	?
12_2002	04 Nov	19:00	07 Nov	20:52	4432	CIR
13_2002	27 Nov	13:00	03 Dec	05:20	8180	CIR
14_2002	26 Dec	08:30	28 Dec	18:25	3475	CIR
01_2003	19 Jan	05:46	23 Jan	05:38	5752	CIR
02_2003	23 Jan	09:44	27 Jan	02:19	5315	?
03_2003	06 Feb	05:22	11 Feb	18:12	7970	CIR
04_2003	16 Feb	05:24	21 Feb	11:10	7546	CIR/ICME
05_2003	04 Mar	10:00	07 Mar	23:34	5134	CIR
06_2003	14 Mar	03:01	19 Mar	21:34	8313	CIR
07_2003	03 Apr	14:11	06 Apr	10:22	4091	CIR?
08_2003	15 Apr	19:10	17 Apr	21:06	2996	CIR
09_2003	20 Apr	15:45	28 Apr	14:31	11447	?
10_2003	01 May	09:00	04 May	14:35	4655	?
11_2003	05 May	08:50	09 May	08:00	5710	CIR/ICME
12_2003	10 May	20:00	16 May	14:23	8303	ICME
13_2003	22 May	09:00	29 May	11:27	10227	CIR?
14_2003	02 Jun	17:00	12 Jun	18:25	14485	ICME/CIR
15_2003	13 Jun	18:58	16 Jun	07:00	3602	ICME/CIR
16_2003	20 Jun	04:53	06 Jul	17:28	23795	ICME/CIR
17_2003	12 Jul	20:00	15 Jul	12:10	3850	CIR
18_2003	18 Jul	16:56	21 Jul	07:51	3775	?
19_2003	27 Jul	09:00	04 Aug	10:46	11628	CIR
20_2003	07 Aug	23:00	14 Aug	11:09	9369	CIR
21_2003	21 Aug	08:00	25 Aug	18:19	6379	CIR

Continued on next page

Table 1 – continued from previous page

Event_Year	Start	UT	Stop	UT	Length (min)	Mechanism
22_2003	10 Sep	08:02	12 Sep	17:39	3457	CIR
23_2003	18 Sep	00:00	22 Sep	20:02	5522	?
24_2003	24 Sep	09:00	27 Sep	01:32	3872	?
25_2003	15 Oct	12:00	22 Oct	18:35	10475	CIR/ICME
26_2003	01 Nov	07:00	04 Nov	06:16	4278	ICME
27_2003	09 Nov	01:41	19 Nov	18:46	15425	ICME/CIR
28_2003	07 Dec	06:32	17 Dec	06:36	14404	CIR
01_2004	01 Jan	04:00	06 Jan	11:11	3868	CIR
02_2004	12 Jan	00:01	15 Jan	05:31	3869	ICME
03_2004	15 Jan	14:06	21 Jan	23:58	3057	CIR
04_2004	29 Jan	09:31	31 Jan	12:28	5811	ICME
05_2004	12 Feb	00:01	16 Feb	00:52	3272	CIR
06_2004	28 Feb	20:10	03 Mar	02:42	4287	?
07_2004	13 Mar	06:05	16 Mar	05:32	4446	CIR
08_2004	06 Apr	08:00	09 Apr	10:06	5445	ICME+CIR
09_2004	02 May	17:57	06 May	12:42	3764	CIR
10_2004	28 May	08:21	31 May	13:44	4644	CIR
11_2004	05 Jun	10:18	10 Jun	07:08	7010	?
12_2004	20 Aug	00:51	23 Aug	09:43	4852	?
13_2004	06 Sep	05:43	08 Sep	14:41	3418	CIR
14_2004	13 Sep	20:04	18 Sep	12:36	6753	ICME
15_2004	03 Oct	05:29	05 Oct	08:40	3071	?
16_2004	12 Oct	21:56	15 Oct	21:10	4275	CIR
17_2004	27 Nov	05:54	01 Dec	12:00	6126	CIR
18_2004	06 Dec	04:54	09 Dec	01:23	4110	?
01_2005	01 Jan	19:07	06 Jan	00:00	6053	CIR?
02_2005	29 Jan	06:13	01 Feb	00:56	4003	CIR
03_2005	07 Feb	22:00	12 Feb	05:24	6204	CIR?
04_2005	07 Mar	02:00	10 Mar	18:02	5282	CIR
05_2005	05 Apr	09:00	07 Apr	16:26	3326	CIR
06_2005	12 Apr	07:00	16 Apr	06:16	5716	CIR
07_2005	30 Apr	03:01	04 May	06:31	5970	CIR
08_2005	11 May	06:55	13 May	17:57	3542	?
09_2005	28 Jul	06:00	30 Jul	09:35	4535	CIR
10_2005	05 Aug	11:52	08 Aug	15:04	4512	CIR
11_2005	02 Nov	22:00	05 Nov	17:12	4032	CIR
12_2005	12 Nov	00:13	14 Nov	22:57	4244	?
13_2005	27 Dec	15:13	30 Dec	09:55	4002	CIR
01_2006	19 Feb	15:40	22 Feb	20:55	4635	CIR

Continued on next page

Table 2: Average and standard deviation of the AE index, and Time of occurrence of HILDCAA* (%) between 1998-2007.

Year	Average (nT)	Sd(nT)	HILDCAA* (%)
1998	207.55	144.72	7.1
1999	218.52	137.73	14.2
2000	235.65	150.70	8.6
2001	202.84	141.98	7.7
2002	216.96	146.85	12.2
2003	328.26	175.83	42.2
2004	220.73	153.03	15.6
2005	225.24	160.05	11.7
2006	151.24	120.15	9.5
2007	130.40	102.26	8.0

Table 1 – continued from previous page

Event_Year	Start	UT	Stop	UT	Length (min)	Mechanism
02_2006	19 Mar	01:24	22 Mar	09:58	4834	CIR
03_2006	15 Apr	00:00	17 Apr	01:48	2988	ICME
04_2006	06 Jun	20:00	11 Jun	17:46	7066	CIR
05_2006	14 Jun	21:47	17 Jun	19:05	4158	CIR
06_2006	20 Aug	15:00	22 Aug	19:20	3140	ICME
07_2006	14 Oct	02:00	16 Oct	23:06	4146	CIR
08_2006	10 Nov	08:00	12 Nov	14:12	3252	CIR
09_2006	23 Nov	16:00	27 Nov	20:25	6025	CIR
10_2006	06 Dec	13:00	09 Dec	04:27	3807	CIR/ICME
11_2006	19 Dec	23:29	24 Dec	00:42	5833	CIR
01_2007	01 Jan	23:03	04 Jan	18:26	4043	CIR
02_2007	16 Jan	09:39	20 Jan	01:58	5299	CIR/ICME?
03_2007	29 Jan	19:00	01 Feb	00:49	3229	CIR
04_2007	27 Feb	08:45	01 Mar	17:07	3382	CIR
05_2007	01 Apr	09:00	03 Apr	11:15	3015	CIR
06_2007	27 Apr	09:48	30 Apr	16:59	4751	CIR
07_2007	23 May	15:00	27 May	20:18	6078	?
08_2007	10 Aug	07:39	12 Aug	12:19	3160	CIR
09_2007	01 Sep	16:31	03 Sep	17:10	2919	CIR
10_2007	05 Sep	00:21	07 Sep	04:43	3142	CIR
11_2007	24 Nov	07:30	26 Nov	11:17	3107	?

Table 3: Mean values of the parameters registered among all 135 HILDCAA* events.

PARAMETERS	AVERAGE $\pm \sigma$
AE (nT)	348.1 ± 67.1
AU (nT)	123.9 ± 34.2
AL (nT)	-224.2 ± 47.3
Dst (nT)	-22.1 ± 9.1
Density (cm^{-3})	4.3 ± 1.3
Temperature (K)	170976.3 ± 58049.9
$ V $ (km/s)	547.1 ± 83.9
Bz (nT)	-0.70 ± 0.88
$ B $ (nT)	6.6 ± 1.2
Pressure (nPa)	2.4 ± 0.6
Beta	0.66 ± 0.27

Table 4: Solar wind parameters related to HILDCAA* events compared with different levels of geomagnetic activity.

Higher values during HILDCAA*			
	Background	HILDCAA*	High Activity (geomagnetic Storm)
Tp(K)	$\approx 1.1 \times 10^5$	$> 1.1 \times 10^5$	$< 1.1 \times 10^5$
V (km/s)	< 400	> 450	≈ 450
Beta		≈ 0.7	$\ll 1$
Intermediates			
Bs (nT)	0	$-2 \leq Bs \leq 0$	< -3
Bo (nT)	≈ 5	$5 < Bo < 9$	> 9
Smaller			
Density (cm^{-3})	≈ 6.1	< 6	$\gg 6$

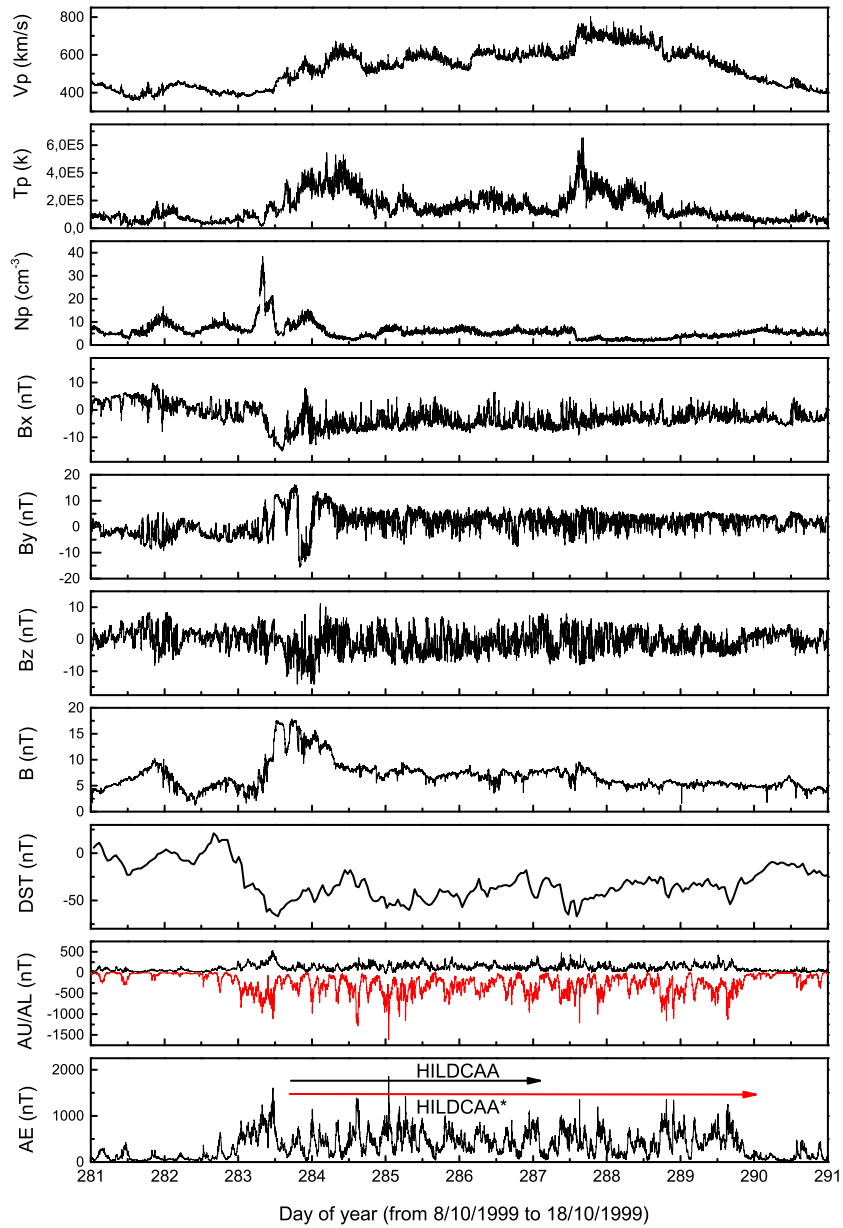


Figure 1: From top to bottom: (a) solar wind speed (V_{sw} in km/s), (b) temperature (K), (c) plasma density (N_{sw} in cm^{-3}), (d) B_x component, (e) B_y component, (f) B_z component in the GSM coordinate system (nT), (g) IMF magnitude (B_0 in nT), (h) Dst index (nT), (i) AU/AL indices (nT), and (j) AE index (nT). Red arrows indicate the interval of the HILDCAA event as defined by [Tsurutani and Gonzalez \(1987\)](#) (beginning at 23:01 of day 10/10 and ending at 17:38 on 14/10), and HILDCAA* event (beginning 23:01 day 10/10 and ending at 07:57 on 18/10).

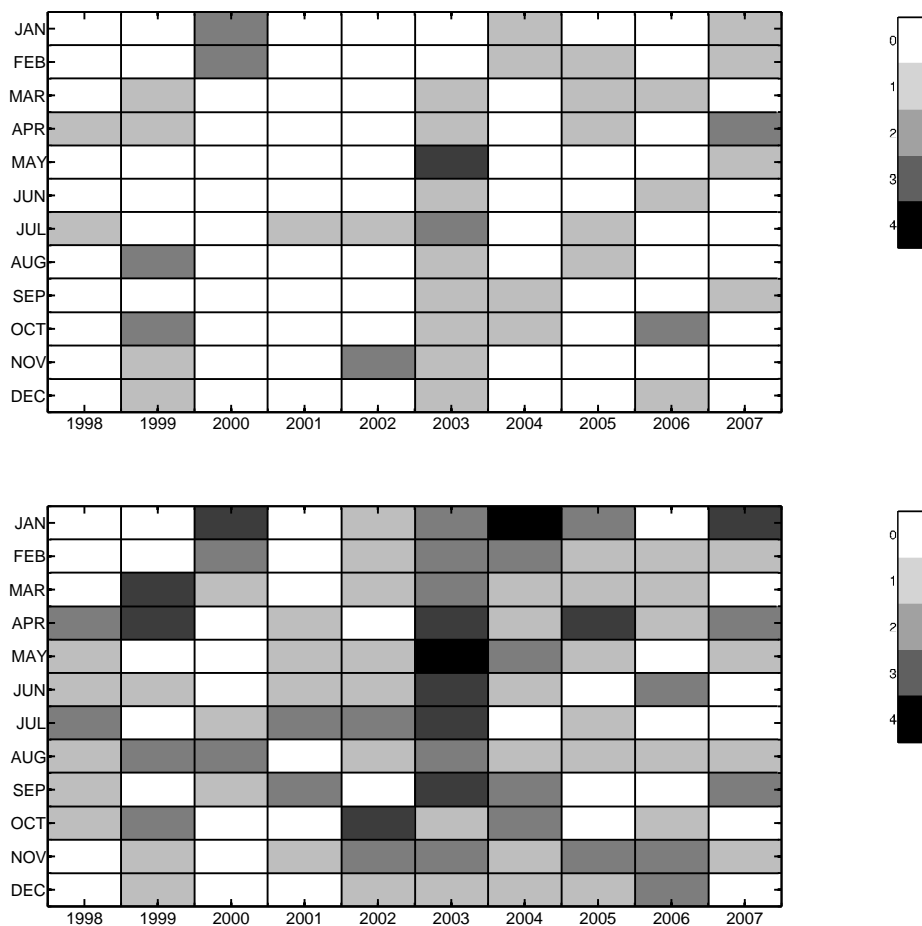


Figure 2: The number of HILDCAAs (top panel) and HILDCAAs* (bottom panel) for the twelve months of the years 1998–2007. The number of events for each month is given by the shades of gray in the legend at the right.

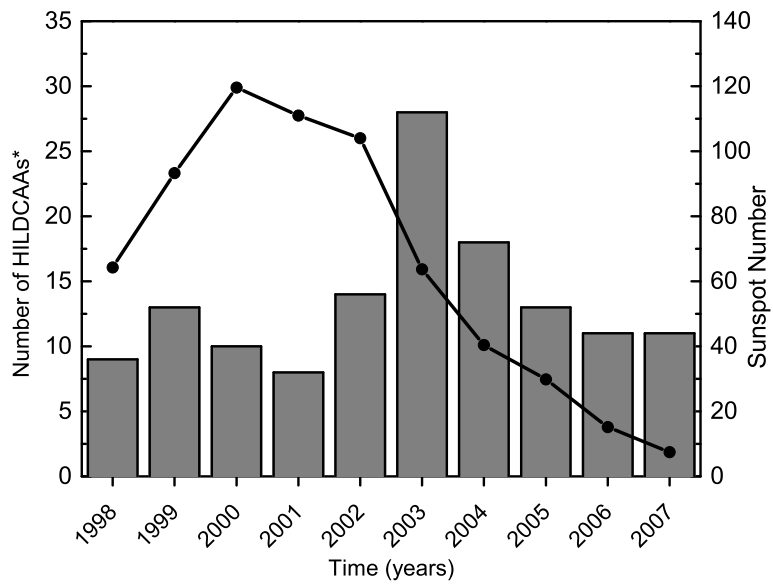


Figure 3: Distribution of HILDCAA* events (bars) and annual averages of sunspot number (line) from 1998 to 2007.

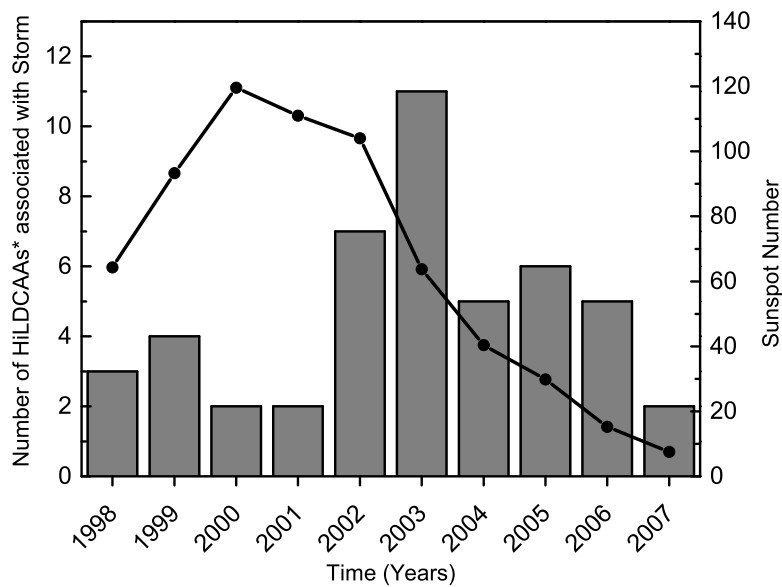


Figure 4: Histogram of the HILDCAA* events associated with geomagnetic storms from 1998 to 2007.

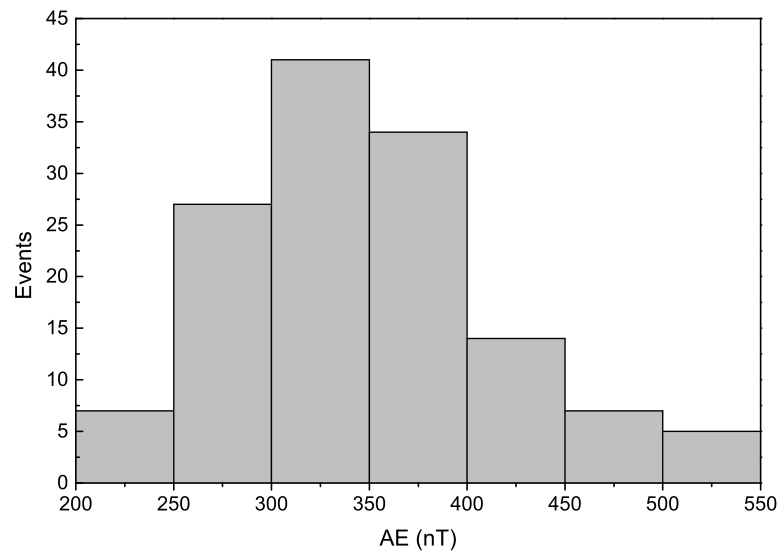


Figure 5: Histogram of the mean values of AE index for 135 HILDCAA* events from 1998 to 2007. Average and standard deviation of the AE index, and Time of occurrence of HILDCAA (%) between 1998-2007.

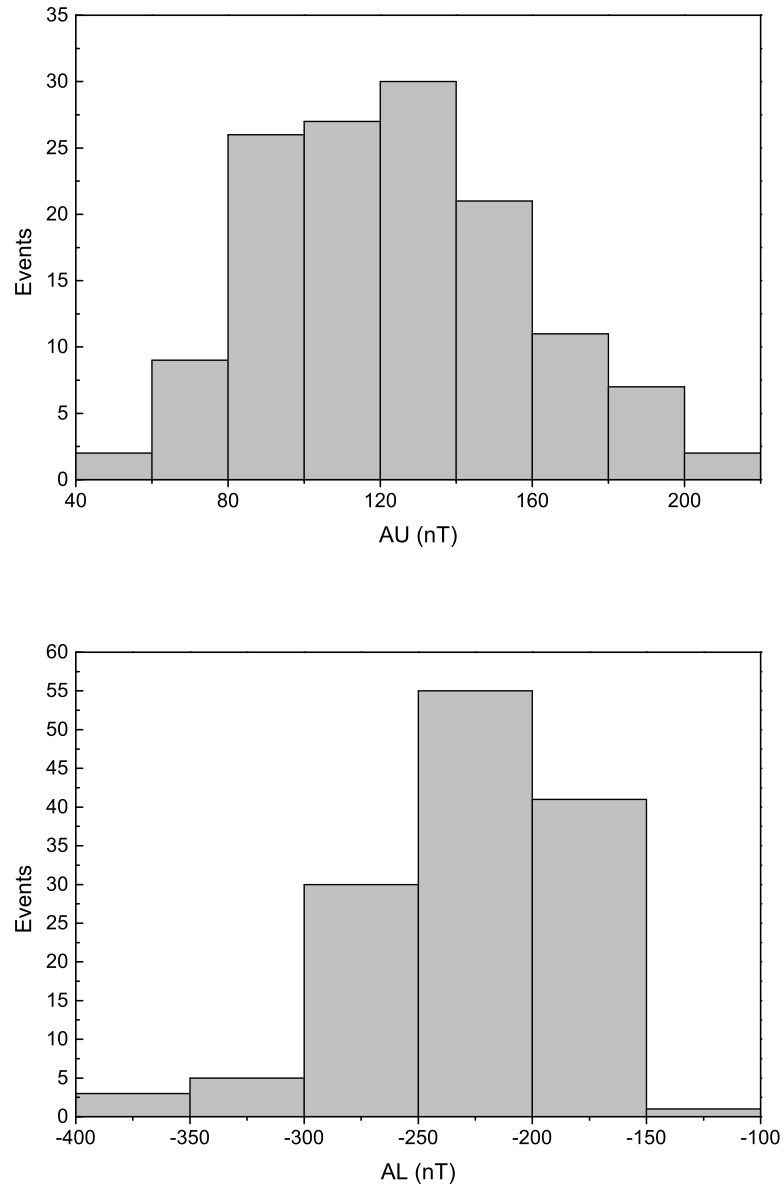


Figure 6: Histogram of the average values of the AU (top panel) and AL (bottom panel) indices for all 135 HILDCAA* events between 1998-2007.

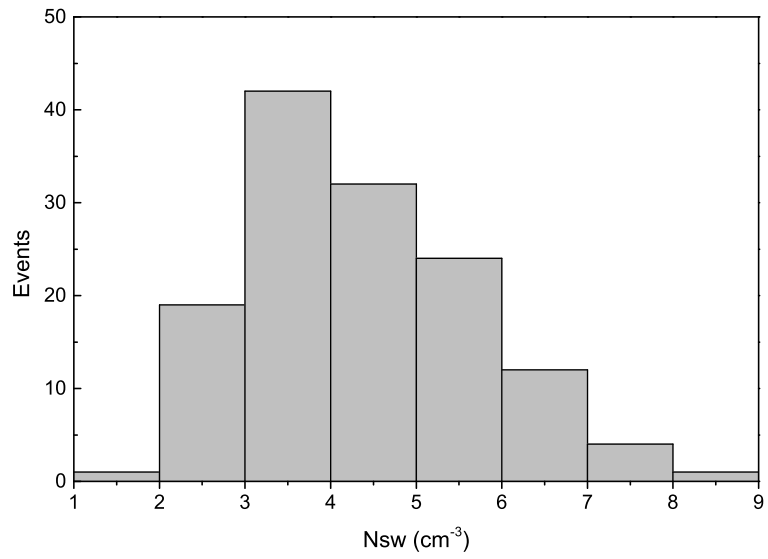


Figure 7: Histogram of the average values of the solar wind proton density for all 135 HILDCAA* events from 1998 to 2007.

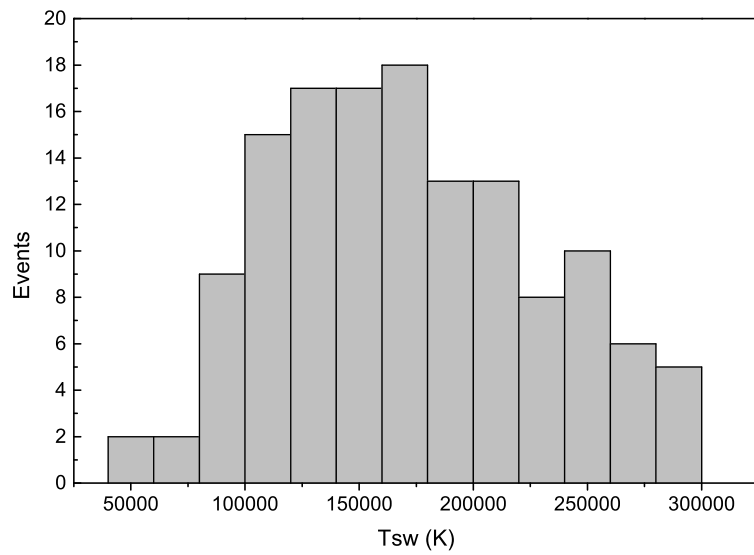


Figure 8: Histogram of the average values of the solar wind proton temperature for all 135 events HILDCAA* 1998-2007.

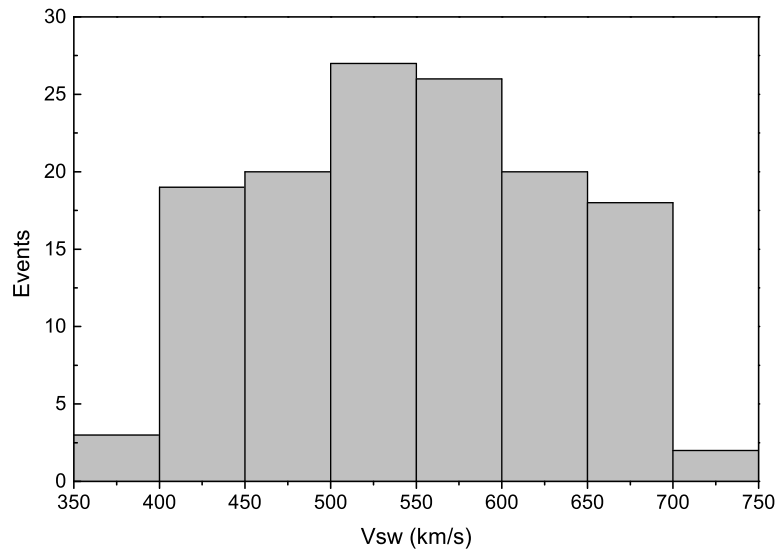


Figure 9: Histogram of the average values of the solar wind speed for all 135 HILDCAA* events from 1998 to 2007.

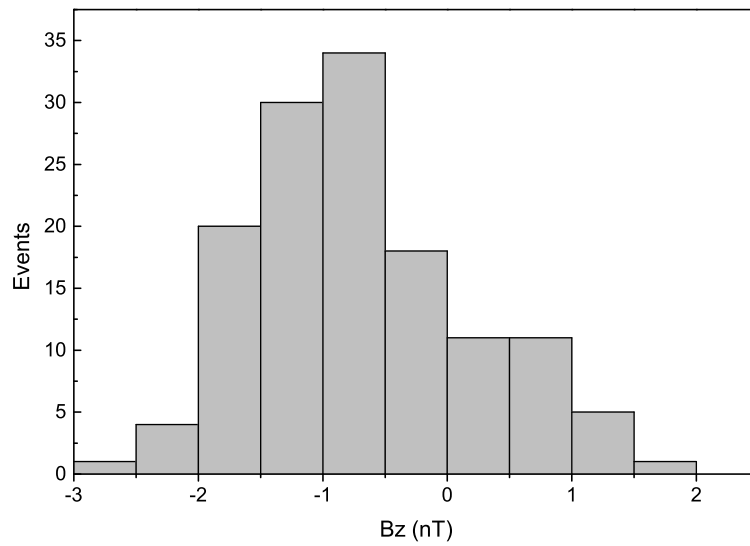


Figure 10: Histogram of the average values of Bz (north-south) component of the interplanetary magnetic field for all 135 events HILDCAA* from 1998 to 2007.

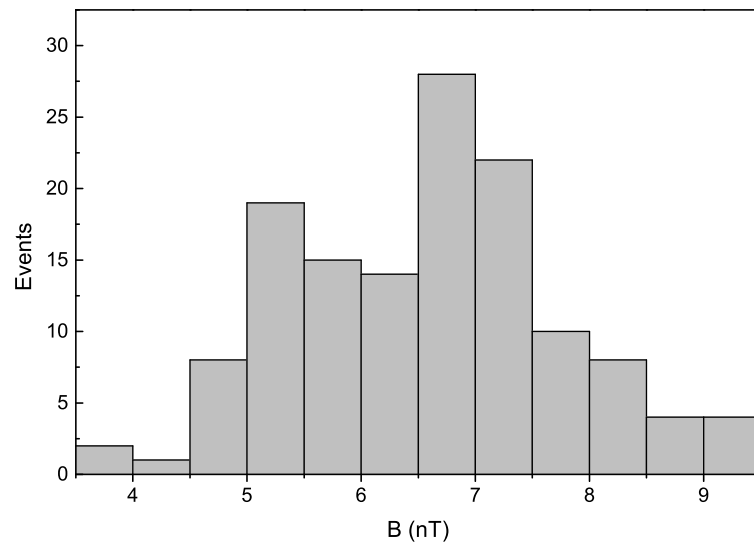


Figure 11: Histogram of the average values of the magnetic field magnitude for all 135 HILDCAA* events from 1998 to 2007.

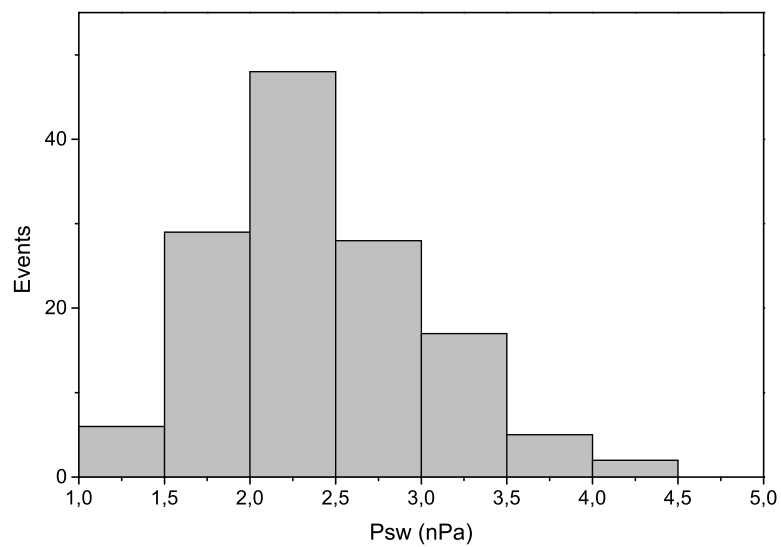


Figure 12: Histogram of the average values of the solar wind dynamic pressure for all 135 HILDCAA* events from 1998 to 2007.

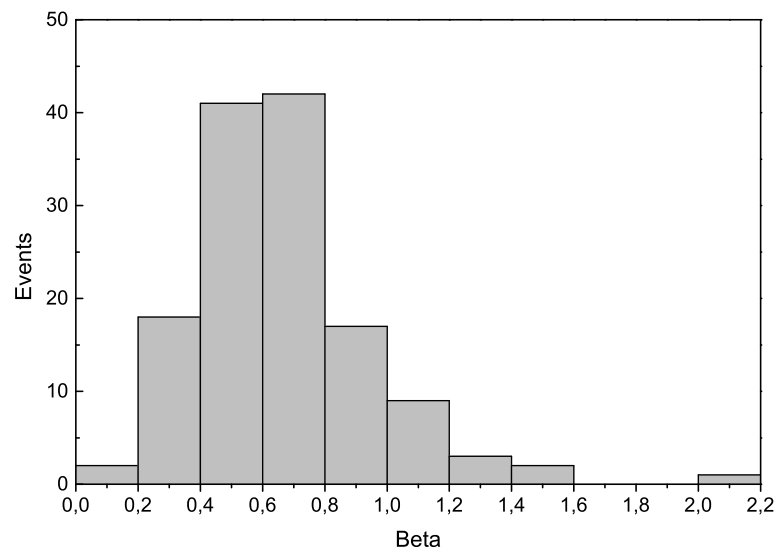


Figure 13: Histogram of the average values of solar wind plasma beta for all 135 HILDCAA* events from 1998 to 2007.